Synthesis and structural characterization of 2-D layered copper(II) styrylphosphonate coordination polymers

Bianca Maranescu[a], Aurelia Visa[a], Gheorghe Ilia[a], Zeno Simon[a], Konstantinos D. Demadis[b], Rosario M.P. Colodrero[c], Aurelio Cabeza[c], Oriol Vallcorba[d], Jordi Rius[d] & Duane Choquesillo-Lazarte[e]

[a] Institute of Chemistry Timişoara of the Romanian Academy, Timişoara, Romania

[b] Crystal Engineering, Growth and Design Laboratory, Department of Chemistry, University of Crete, Heraklion, Greece

[c] Departamento de Química Inorgánica, Universidad de Málaga, Málaga, Spain

[d] Institut de Ciència de Materials de Barcelona, Barcelona, Spain

[e] Laboratorio de Estudios Cristalográficos, IACT-CSIC, Granada, Spain

Accepted author version posted online: 28 May 2014.Published online: 19 Jun 2014.

PLEASE SCROLL DOWN FOR ARTICLE

Taylor & Francis
Taylor & Francis Group

Synthesis and structural characterization of 2-D layered copper(II) styrylphosphonate coordination polymers

BIANCA MARANESCU†, AURELIA VISA*†, GHEORGHE ILIA†, ZENO SIMON†,
KONSTANTINOS D. DEMADIS*‡, ROSARIO M.P. COLODRERO§,
AURELIO CABEZA§, ORIOL VALLCORBA¶, JORDI RIUS¶ and
DUANE CHOQUESILLO-LAZARTE‖

†Institute of Chemistry Timişoara of the Romanian Academy, Timişoara, Romania
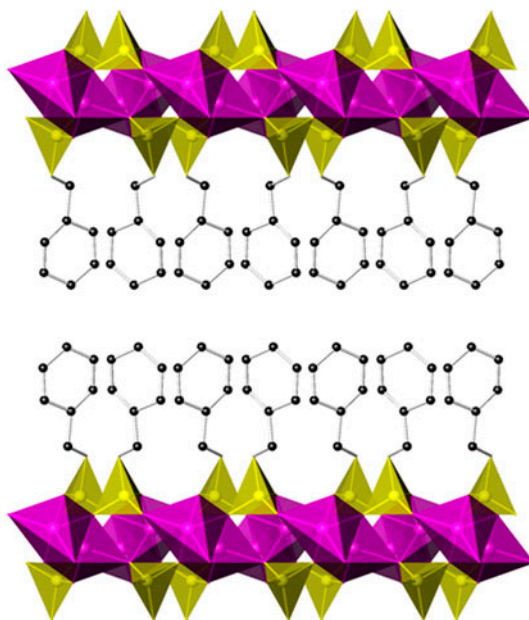‡Crystal Engineering, Growth and Design Laboratory, Department of Chemistry, University of Crete,
Heraklion, Greece
§Departamento de Química Inorgánica, Universidad de Málaga, Málaga, Spain
¶Institut de Ciència de Materials de Barcelona, Barcelona, Spain
‖Laboratorio de Estudios Cristalográficos, IACT-CSIC, Granada, Spain

*Corresponding authors. Email: avisa@acad-icht.tm.edu.ro (A. Visa); demadis@chemistry.uoc.gr (K.D. Demadis)

We report the synthesis, physicochemical characterization, and crystal structure of Cu-SP (SP = styrylphosphonic acid, $H_2O_3PCH=CH_2(C_6H_5)$), the first reported example of a metal derivative of SP. The starting SP acid was fully characterized by X-ray single-crystal diffractometry, elemental analysis (C and H), ^{31}P-NMR, ^{13}C-NMR, ^{1}H-NMR, HPLC, UV–vis, MS, TG, and FT-IR spectroscopy. The copper(II) derivative was synthesized and characterized by DTA-TG and FT-IR, and also its structure was determined from powder data. The crystal structure was refined by the Rietveld method. The crystal structure of Cu-SP shows a layered 2-D architecture, where the organic moieties are pointed toward the interlamellar space. The inorganic layers are composed of Cu^{2+} dimers, where the coordination geometry of Cu^{2+} can be described as distorted trigonal bipyramid. The three coplanar oxygens (O2, O3, and O3) have bond distances of 2.165(9), 1.982(9), and 2.103(11) Å, respectively. The bond lengths for the apical oxygens (O1 and O2) are 1.908(13) and 1.996(11) Å, respectively.

Keywords: Styrylphosphonic acid; Metal phosphonates; Copper; MOF; Layered compounds; Unsaturated phosphonates

1. Introduction

The need for new and improved properties has been a driving force for the development of new materials and technologies beyond those available for conventional materials. Organic–inorganic hybrid compounds are an important class of materials, which has gained dramatic momentum in the last 15 years [1]. The growing interest is due to potential applications in gas adsorption [2], magnetism [3], catalysis [4], and others. Access to such materials requires extensive synthetic efforts, which are based principally on the availability of new organic linkers. One such family of linkers embraces phosphonic acids [5]. Metal phosphonate frameworks have attracted considerable attention lately for a number of reasons. The materials generally display high thermal and hydrolytic stability and readily form in water or organic solvent/water mixtures. The materials also present admirable structural variability, which largely depends on synthesis conditions, primarily temperature and pH. Physical and chemical properties were investigated to identify potential for gas storage, pharmaceutics, surface protection, and optoelectronic devices or sensor applications [6].

Our aim is to synthesize and characterize new metal organic frameworks (MOFs) containing organic linkers which possess phosphonic groups. The starting point of this work was the synthesis of the styrylphosphonic acid (SP) [7] as a precursor with good potential for structural flexibility and network topology of synthesized MOFs [8]. Herein, we report the synthesis, physicochemical, and structural characterization of the first metal derivative of SP, CuSP, $[Cu(CH_2=C(C_6H_5)PO_3)H_2O]_n$.

2. Experimental

2.1. *Materials*

All reagents were purchased from Sigma-Aldrich and used without purification, except the double-distilled water, which was produced in-house.

2.2. *Synthesis of SP*

A toluene solution of styrene (100 mM in 20 mL toluene) was introduced into a three-necked 100-mL round-bottomed flask. This flask was fitted with a reflux condenser, a thermometer, and a dropping funnel and was filled with nitrogen. The mixture was heated at

60 °C. Next, 100 mM phosphorus pentachloride dissolved in 20 mL toluene was added dropwise over one hour while maintaining the reaction temperature between 60 and 70 °C. Agitation is maintained at this temperature until a clear solution is formed. The byproduct HCl gas was removed from the reaction mixture through an absorption scrubber. The toluene was distilled under vacuum while maintaining the temperature under 60 °C. The resulting mixture was finally hydrolyzed in 5 mL bidistilled water and SP acid precipitated as white–yellow crystals. The crystals were filtered, dried, and recrystallized from a 1:5 mixture of EtOH and H_2O. ^{1}H-NMR (400 MHz, $CDCl_3$): 2.077 ppm P–OH, 6.48 (dd, $^3J_{HH}$ = 16.8 Hz, H-1), 7.20 ppm (dd, $^3J_{HH}$ = 17.6 Hz, H-2), 7.3–7.5 ppm (m, H-5, H-6), 7.5–7.7 ppm (m, H-4); ^{31}P-NMR (162 MHz, $CDCl_3$): 13.44 ppm; ^{13}C-NMR (100 MHz, $CDCl_3$): 120.88 ppm (s, C1), 127.83 ppm (s, C6), 129.3 ppm (s, C4), 129.92 (s, C5), 135.75 ppm (d, $^3J_{CP}$ = 46.2 Hz, C3), and 143.45 ppm (d, $^2J_{CP}$ = 11.8 Hz, C2).

2.3. Synthesis of copper styrylphosphonate

A 100 mL round-bottomed flask was charged with Cu^{2+} salt (sulfate or nitrate, 50.0 mM), SP (50.0 mM), urea (50.0 mM), and distilled water (50 mL). The pH was adjusted to 2.8 with an aqueous solution of NaOH (0.1 M). The solution was heated in an oil-bath at 80 °C for 75 h. The resulting crystals were collected by filtration, washed with distilled water, and dried in air (yield: 60–80%) [12]. Elemental analysis: $Cu(O_3PCH=CH_2(C_6H_5))$ (M.W. = 245.67 g M^{-1}): Calcd: C, 39.11%; H, 2.87%, found: C, 38.75%; H, 2.49%.

2.4. Instrumentation

Elemental analyses (CHN) were measured on a Perkin–Elmer 240 analyzer or a CE-440 Elemental Analyzer, Exeter Analytical Inc. Thermal analysis (TG-DTA) data were recorded on an SDT-Q600 analyzer from TA instruments. The temperature was varied from RT to 800 °C at a heating rate of 10 °C min^{-1}. Alternatively, a Perkin–Elmer Diamond thermogravimetric analyzer was used from 30 to 700 °C under a flow of N_2 with a heating rate of 10 °C/min. Measurements were carried out on a sample in an open platinum crucible under a flow of air. NMR spectra were recorded with a Bruker DRX 400 MHz spectrometer. The HPLC system used in this work was a Jasco PU-1580 solvent delivery system and a MD-1510 UV/vis detector, with a 10 μL flow cell. A reversed-phase Nucleosil C18 column (25 cm × 0.4 mm, microparticle size) was used for separation. A Reodyne 7725 injector with a 10 μL external loop was used for sample introduction. A Borwin Chromatography workstation was used to control the operation of HPLC, to obtain the chromatogram, and perform data processing. MS spectra were recorded with a Bruker Daltonik Esquire 6000 equipped with ESI (Electrospray ionization). UV–vis spectra were performed with a CECIL CE 720 spectrometer in methanol from 190 to 900 nm. FT-IR spectra were recorded on a Jasco-FT/IR-4200 instrument from 400 to 4000 cm^{-1} using KBr pellets. The pH was measured using a pH HI 2221 Calibration Check pH/ORP Meter by Hanna Instruments.

2.5. Structural characterization

Laboratory X-ray powder diffraction (XRPD) pattern for copper styrylphosphonate (Cu-SP) was recorded in flat-sample transmission geometry on an EMPYREAN diffractometer

(PANalytical B.V.) equipped with a θ/θ goniometer, CuK$\alpha_{1,2}$ radiation ($\lambda = 1.542$ Å), and a focusing mirror. This PreFIX optical component is capable of converting the divergent beam into a convergent radiation focused on the goniometer circle. The EMPYREAN diffractometer was equipped with fixed incident and diffracted beam anti-scatter slits of ¼° and 5 mm, respectively. The detector was PIXCEL 3-D RTMS, which comprises more than 65,000 pixels, each 55×55 microns in size, each having its own circuitry. Powder samples were placed in the holders between two Kapton films. The cylindrical sample diameter and thickness were ~10.0 and ~0.3 mm, respectively. The overall measurement time was ~3 h per pattern to have very good statistics over the 2θ range of 3–80° with 0.0131° step size (2θ). It must be noted that the strongly preferred orientation shown by this layered solid prevented the structural resolution from diffraction data collected in the Bragg–Brentano reflection configuration even after disordering the sample with spherical amorphous nanoparticles of silica gel Cab-o-sil M5 (from Fluka) to the minimization of this effect as previously reported [9].

The powder pattern was indexed with DICVOL06 [10]. The refinement of the unit cell parameters, the identification of the space group, and the extraction of intensities for structure solution was performed with DAJUST software [11]. The crystal structure was solved with the direct-space strategy implemented in TALP [12], taking a Cu and the molecule of phosphonic acid (with the restraints taken from the available single crystal structure of this compound) as starting fragments. The resulting crystal structure model gave a poor figure of merit due to the presence of severe preferred orientation in the sample which was modeled with the March–Dollase correction [13], in the subsequent Rietveld refinement with the GSAS package [14], and the EXPGUI graphic interface [15]. In spite of the poor figure of merit of TALP, the correct solution could be easily discriminated (71% successful trials). The crystal structure was refined by the Rietveld method [16] using soft constraints to maintain chemically reasonable geometries for the phosphonate and alkyl chain. The following soft constraints were imposed in order to preserve chemically reasonable geometries for the phosphonate, alkyl chain, and amine groups. The soft constraints were:/PO$_3$C tetrahedron/P–O (1.53(1) Å), P–C (1.80(1) Å), O···O (2.55(2) Å), O···C (2.73(2) Å), /Csp^2–Csp^2, and Csp^2–Csp^3/C=C (1.33(1) Å), C–C (1.50(1) Å) and/aryl/aromatic ring/C–C (1.40(1) Å), C$_{ring}$···C$_{ring}$ (2.40(1) Å), C$_{ring}$···C$_{ring}$ (2.78(1) Å). The final weight for the soft constraints was 30. No attempts to locate hydrogens were carried out due to the limited quality of the XRPD data. Crystallographic data and refinement details are: space group P 2$_1$/c; $a = 18.9739(11)$ Å; $b = 5.6880(1)$ Å; $c = 7.5969(2)$ Å; $\beta = 98.765(3)°$; $\alpha = \gamma = 90°$; $V = 810.32(6)$ Å^3; $Z = 4$; data/restraints/parameters = 5948/29/91; $R_{wp} = 0.1555$; $R_p = 0.1138$; $R_F = 0.0762$; CCDC Reference Code = 977,399 (see table S-1 in the Supplementary material, see online at http://dx.doi.org/10.1080/00958972.2014.928289).

A single crystal of SP was handled under inert conditions and immersed in perfluoropolyether as protecting oil for manipulation and then it was mounted on a MiTeGen Micromounts^{TM} for subsequent data collection. Data were collected with a Bruker X8 Proteum diffractometer. Data were processed with APEX2 [17] and corrected for absorption using SADABS [18]. The structure was solved by direct methods [19], which revealed the position of all non-hydrogen atoms. These atoms were refined on F^2 by a full-matrix least-squares procedure using anisotropic displacement parameters [19]. All hydrogens were located in difference Fourier maps and included as fixed contributions riding on attached atoms with isotropic thermal displacement parameters 1.2 times those of the respective atom. Crystallographic data are given in table S-2 (Supplementary material).

3. Results and discussion

3.1. *Characterization of SP*

During the writing of this work, we discovered that the crystal structure of SP was published [20]. Hence, we will not provide any extensive discussion on molecular structure. Basically, the structure is two conformational isomers where the oxygen of the phosphoryl group takes part in formation of two intermolecular hydrogen bonds: one between molecules of the same type and one between molecules of different types [21]. We have placed all crystallographic data in the Supplementary material. However, since other physicochemical characterization on SP is lacking, we provide these data herein.

SP was characterized by the following physicochemical methods: X-ray single crystal diffractometry, elemental analysis (C and H), ^{31}P-NMR, ^{13}C-NMR, ^{1}H-NMR, HPLC, UV–vis, MS, TG, and IR spectroscopy. The structure of SP (scheme 1) was confirmed by ^{1}H, ^{13}C-NMR, ^{31}P-NMR, and COSY spectra (figure 1). All spectra were recorded in deuterated chloroform at 298 K. All chemical shifts were measured using the XSI scale and TMS as internal standard [22].

The 2-D homonuclear correlation spectrum (COSY) shows one cross-peak between aromatic hydrogens at 7–8 ppm, one cross-peak between vinyl hydrogens at 6–7 ppm, as well as a cross-peak between P–OH and the H_2O present in the sample at 4.78 ppm.

The purity of SP was also confirmed by HPLC in isocratic elution mode, recording a major peak at $t_r = 2.640$ min (figure 2, upper). Mass spectrometry revealed very clearly in both modes (MS+) and (MS−) the molecular peaks of the synthesized SP acid. Molecular peaks were used as the reference peaks ($m/z = 182$) (figure 2, lower).

The analysis by UV–vis spectrophotometry of the SP acid in methanol shows a maximum absorption at $\lambda = 250$ nm, due to the aromatic ring $\pi–\pi^*$ transitions (see Supplementary material). The FT-IR spectra of the SP acid (see Supplementary material) shows a broad band corresponding to the P–OH stretch at 2200–3000 cm^{-1}. Bands assigned to C=C bonds of the aromatic ring appear at 1650–1550 cm^{-1}. P=O and PO_3 stretching vibrations appear at 1350–950 cm^{-1}. Lastly, two weak bands at 686 and 738 cm^{-1} are assigned to the vinyl moiety.

Thermal analysis performed on crystals of SP shows a weight loss around 170 °C. This transformation can be attributed to loss of water and melting of acid. A second mass loss at ~280 °C is associated with a polymerization process followed by a thermal degradation process. Above 500 °C the phenyl moiety decomposes. At the end of the degradation process at 700 °C the mass loss amounts to 72.48%.
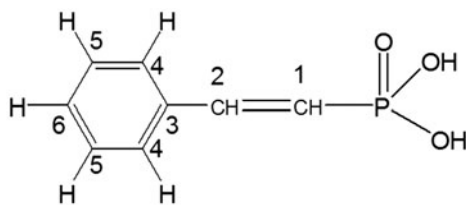
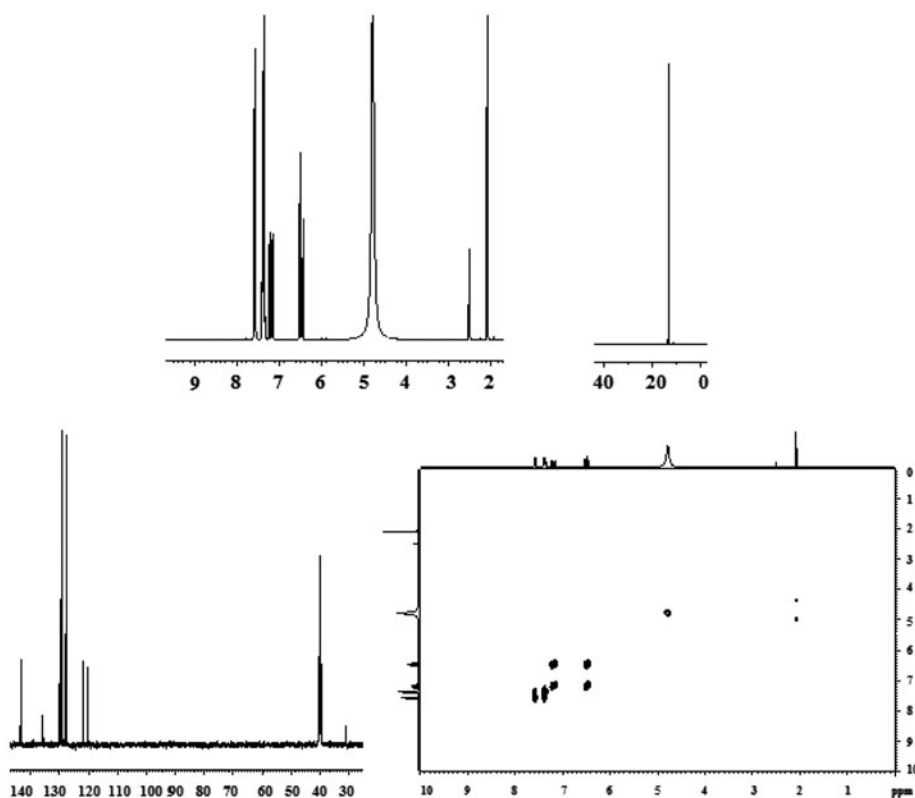Scheme 1.   Styryl phosphonic acid atom numbering.

Figure 1.   Upper left: ^{1}H-NMR of SP. Upper right: ^{31}P-NMR of SP. Lower left: ^{13}C-NMR of SP. Lower right: 2-D homonuclear correlation spectroscopy (COSY) for SP. All axes are in "ppm".

3.2. *Synthesis, characterization, and structure of Cu-SP*

Reaction parameters like molar ratio, pH, and temperature were varied in order to establish the optimum conditions for synthesis of Cu-SP. The pH was adjusted in the range 1–3 by adding stepwise a 0.1 M NaOH solution. The reactant mixture was kept for 72 h at 70–85 °C. Optimum synthesis conditions were found to be: temperature 80 °C, Cu : SP molar ratio 1:1, and pH 2.8. The product is a microcrystalline powder of high crystallinity, as indicated by its XRPD pattern (see Supplementary material).

Thermogravimetric analysis for Cu-SP (figure 3) confirms the crystallization of the solid without lattice water. The DTA-TG curves only show a strong endothermic process centered at 320 °C corresponding to combustion of the ligand with an associate weight loss of 39.06%, which agrees well with the calculated weight loss for formation of $Cu_2P_2O_7$ (38.72%), although we could not indentify it by powder X-ray diffraction

The crystal structure of $Cu(O_3PC=CHC_6H_5)$, Cu-SP, was refined by the Rietveld method using soft constraints to maintain chemically reasonable geometries for the phosphonate and the alkyl chain (see figure 4). The structure reveals a layered 2-D architecture, where the organic moieties are pointed toward the interlamellar space. The inorganic layers are composed of Cu^{2+} dimers, where the coordination geometry of Cu^{2+} can be described as a distorted trigonal bipyramid (figure 5). The three coplanar oxygens (O2, O3, and O3) have
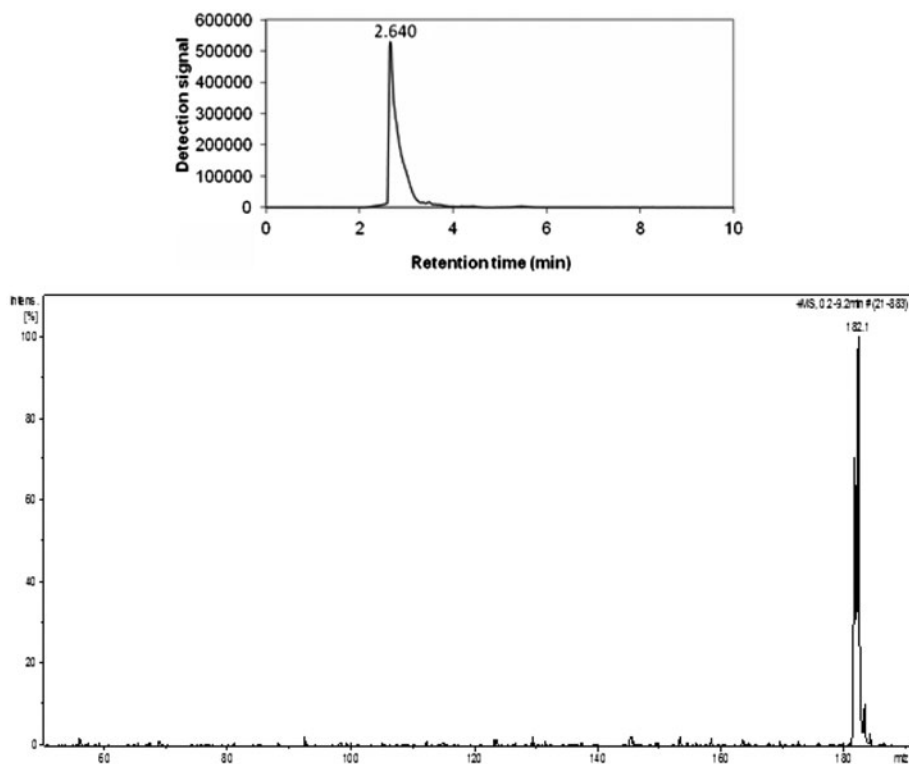
Figure 2.   Upper: chromatogram of the SP (methanol isocratic elution $v = 1$ mL min^{-1}). Lower: mass spectrum (MS+) of SP acid ($m/z = 182$). 2-D homonuclear correlation spectroscopy (COSY) for SP. All axes are in "ppm".
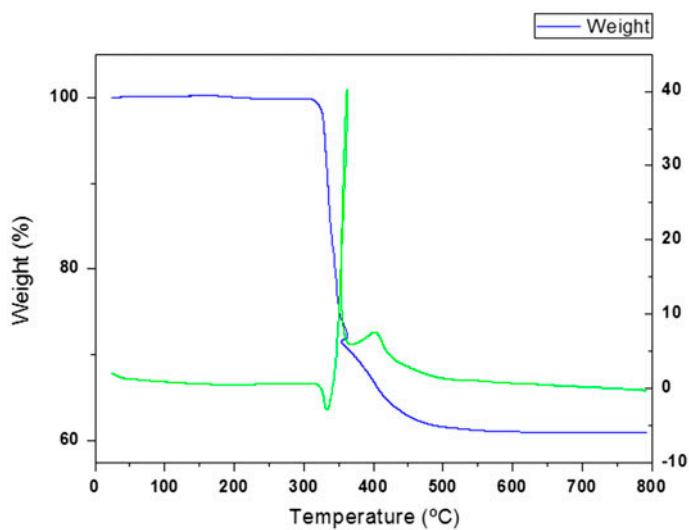

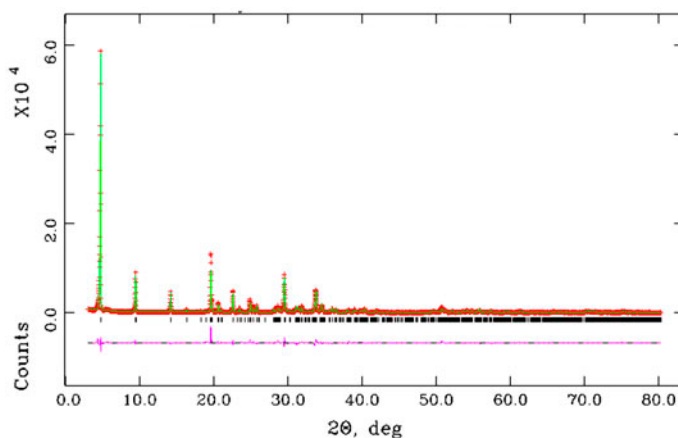Figure 3.   Thermogravimetric analysis of Cu-SP.

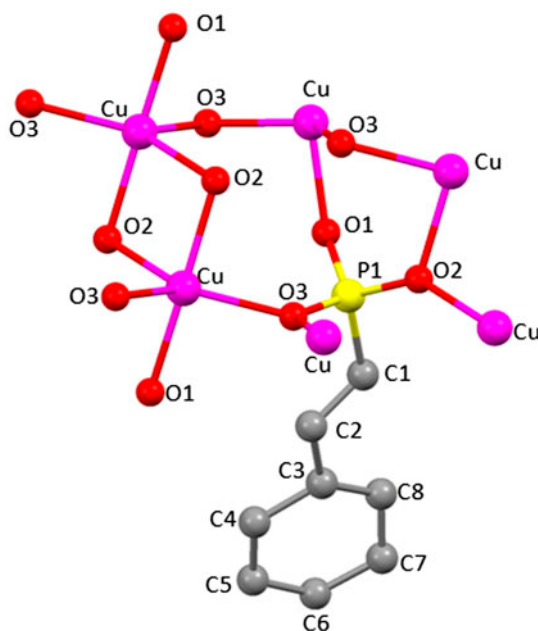Figure 4. Rietveld plot for Cu(O3PC=CHC6H5), Cu-SP.

Figure 5. Copper coordination environment and connectivity of the phosphonate group. Color codes: Cu, magenta; P, yellow; O, red; C, grey (see http://dx.doi.org/10.1080/00958972.2014.928289 for color version).

bond distances between 2.165(9), 1.982(9), and 2.103(11) Å, respectively. The bond lengths for the apical oxygens (O1 and O2) are 1.908(13) and 1.996(11) Å, respectively. The geometry for copper, although less common than square pyramidal [23], has already been described for other copper phosphonates and the observed bond lengths and angles are consistent with previous examples given in the literature [24].

The three oxygens of the phosphonate are all bonded to Cu. Oxygen O1 is coordinated to a copper atom in a terminal fashion, while O2 and O3 bridge two coppers forming six- and
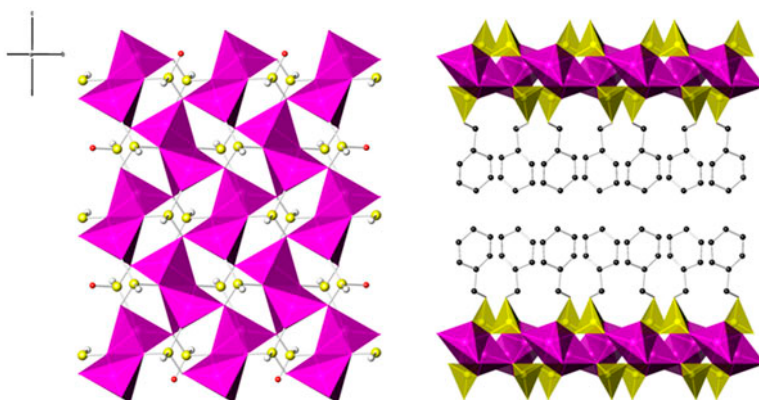
Figure 6. (left) View along the *a*-axis and (right) packing of the layers along the *a*-axis (*b*-axis in horizontal). O3PC tetrahedra, yellow; MO5 trigonal bipyramid, pink; Cu, pink; P, yellow; O, red; C, black (see http://dx.doi.org/10.1080/00958972.2014.928289 for color version).

eight-membered rings. The inorganic layers (plane *bc*) result from linking of copper dimeric units to each other by corner sharing (figure 6). It must be emphasized that the connectivity is the same as found for $Cu(O_3PCH_2CH_3)$ [24(b)]. The phosphonates are arranged alternatively over and below the inorganic layers with the organic moieties projecting into the interlayer region. The adjacent organic moieties in a layer are oriented such that each phenyl ring is nearly perpendicular to two others at 3.86 and 3.96 Å as observed for copper phenylphosphonate [24(a)] and the Na salt of SP [25]. Thus, the layers are held together by van der Waals interactions. The absence of any π–π stacking interactions between the phenyl rings that originate from the same layer must be noted. The adjacent rings are tilted ~65° from each other (see figure 7).
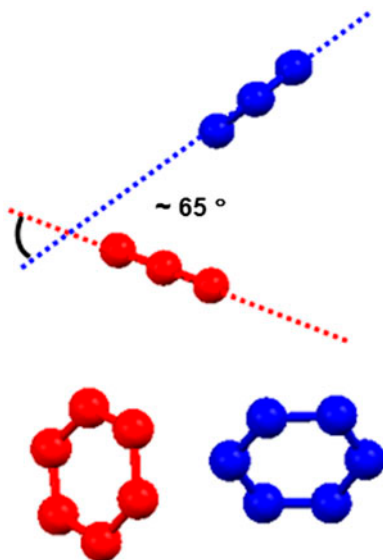

Figure 7. Disposition of the phenyl rings from adjacent SP ligands, from the same layer.

The crystal structure of Cu-SP resembles that of Na-SP [25]. Although the structures differ in the way the inorganic layers are built. Thus, Na^+ cations show distorted octahedral coordination environments and the layers are composed of chains of Na_2O_{10} dimers connected to each other by edge sharing and through the phosphonic groups.

4. Conclusion

We report the synthesis, characterization, and crystal structure of Cu-SP (SP = styrylphosphonic acid, $H_2O_3PCH=CH_2(C_6H_5)$), the first reported example of a metal salt of SP. Cu-SP was synthesized and characterized by DTA-TG and FT-IR, and also its structure was determined from powder data. The crystal structure of Cu-SP shows a layered 2-D architecture, where the organic moieties are pointed toward the interlamellar space. The inorganic layers are composed of Cu^{2+} dimers, where the coordination geometry of Cu^{2+} can be described as a distorted trigonal bipyramid. This is a follow-up on our on-going research with unsaturated phosphonic acids and derivatives [26].

Acknowledgments

Funding

References

[1] (a) *Chem. Rev.*, **112**, 673 (2012); (b) *Chem. Soc. Rev.*, **40**, 453 (2011); (c) *Chem. Soc. Rev.*, **38**, 1201 (2009); (d) D. Farrusseng. *Metal-organic Frameworks. Applications from Catalysis to Gas Storage*, Wiley-VCH Verlag & Co. KGaA, Weinheim (2011); (e) L. MacGillivray. *Metal-organic Frameworks. Design and Application*, Wiley-VCH Verlag & Co. KGaA, Weinheim (2011).

[2] (a) L.Q. Ma, W.B. Lin. In *Functional Metal-organic Frameworks: Gas Storage, Separation and Catalysis*, M. Schroder (Ed.), *Topics in Current Chemistry*, Vol. 293, pp. 175–205, Wiley-VCH Verlag & Co. KGaA, Weinheim (2010); (b) S. Ma, D. Yuan, X.-S. Wang, H.-C. Zhou. *Inorg. Chem.*, **48**, 2072 (2009); (c) T. Devic, C. Serre, N. Audebrand, J. Marrot, G. Férey. *J. Am. Chem. Soc.*, **127**, 12788 (2005); (d) B.D. Chandler, J.O. Yu, D.T. Cramb, G.K.H. Shimizu. *Chem. Mater.*, **19**, 4467 (2007); (e) L. Hamon, N. Heymans, P.L. Llewellyn, V. Guillerm, A. Ghoufi, S. Vaesen, G. Maurin, C. Serre, G. De Weireld, G.D. Pirngruber. *Dalton Trans.*, 4052 (2012).

[3] (a) J. Kido, Y. Okamoto. *Chem. Rev.*, **102**, 2357 (2002); (b) N. Marques, A. Sella, J. Takats. *Chem. Rev.*, **102**, 2137 (2002); (c) F.A.A. Paz, J. Klinowski, S.M.F. Vilela, J.P.C. Tome, J.A.S. Cavaleiro, J. Rocha. *Chem. Soc. Rev.*, **41**, 1088 (2012); (d) W. Zhang, R.-G. Xiong. *Chem. Rev.*, **112**, 1163 (2012); (e) X. Guo, G. Zhu, Z. Li, Y. Chen, X. Li, S. Qiu. *Inorg. Chem.*, **45**, 4065 (2006).

[4] (a) L.Q. Ma, C. Abney, W.B. Lin. *Chem. Soc. Rev.*, **38**, 1248 (2009); (b) L. Cunha-Silva, S. Lima, D. Ananias, P. Silva, L. Mafra, L.D. Carlos, M. Pillinger, A.A. Valente, F.A.A. Paz, J. Rocha. *J. Mater. Chem.*, **19**, 2618 (2009); (c) F.G. Cirujano, F.X. Llabrés i Xamena, A. Corma. *Dalton Trans.*, 4249 (2012); (d) J. Crassous. *Chem. Soc. Rev.*, **38**, 830 (2009).

[5] K. Popov, H. Rönkkömäki, L.H.J. Lajunen. *Pure Appl. Chem.*, **73**, 1641 (2001).

[6] (a) A. Clearfield, K.D. Demadis. *Metal Phosphonate Chemistry: From Synthesis to Applications*, Royal Society of Chemistry, London (2012) and references therein; (b) D.I. Arnold, X. Ouyang, A. Clearfield. *Chem.*

Mater., **14**, 2020 (2002); (c) D. Kong, J. Zoñ, J. McBee, A. Clearfield. *Inorg. Chem.*, **45**, 977 (2006); (d) G. Alberti, U. Costantino, S. Alluli, N. Tomassini. *Inorg. Nucl. Chem.*, **40**, 1113 (1978); (e) A. Vioux, J. LeBideau, P.H. Mutin, D. Leclerq. *Top. Curr. Chem.*, **232**, 145 (2004); (f) A. Clearfield. *Dalton Trans.*, 6089 (2008); (g) K.D. Demadis, S.D. Katarachia, H. Zhao, R.G. Raptis, P. Baran. *Cryst. Growth Des.*, **6**, 836 (2006); (h) E. Barouda, K.D. Demadis, S. Freeman, F. Jones, M.I. Ogden. *Cryst. Growth Des.*, **7**, 321 (2007).

[7] (a) E. Mascaro, O.I. Pieroni, B.M. Vuano, A.E. Ciolino. *Mol. Med. Chem.*, **13**, 36 (2007); (b) P.C. Schulz, B.S. Fernández-Band, B. Vuano, M. Palomeque, A.L. Allan. *Colloid Polym. Sci.*, **274**, 741 (1996).

[8] (a) D.A. Knight, V. Kim, R.J. Butcher, B.A. Harper, T.L. Schull. *J. Chem. Soc., Dalton Trans.*, 824 (2002); (b) L.K.B. Congiardo, J.T. Mague, A.R. Funk, R. Yngard, D.A. Knight. *Acta Cryst.*, **E67**, m450 (2011); (c) M. Alfred, H. Tesmann, US Patent 4324740 (1982).

[9] A. Cabeza, E.R. Losilla, H.S. Martínez-Tapia, S. Bruque, M.A.G. Aranda. *Adv. X-Ray Anal.*, **42**, 228 (2000).

[10] A. Boultif, D. Louër. *J. Appl. Crystallogr.*, **37**, 724 (2004).

[11] O. Vallcorba, J. Rius, C. Frontera, I. Peral, C. Miravitlles. *J. Appl. Crystallogr.*, **45**, 844 (2012).

[12] O. Vallcorba, J. Rius, C. Frontera, C. Miravitlles. *J. Appl. Crystallogr.*, **45**, 1270 (2012).

[13] W.A. Dollase. *J. Appl. Crystallogr.*, **19**, 267 (1986).

[14] A.C. Larson, R.B. Von Dreele. *General Structure Analysis System (GSAS)*, Los Alamos National Laboratory Report LAUR 86 (2004).

[15] B.H. Toby. *J. Appl. Crystallogr.*, **34**, 210 (2001).

[16] H.M. Rietveld. *J. Appl. Crystallogr.*, **2**, 65 (1969).

[17] Bruker. *APEX2 Software, V2013.2*, Bruker AXS Inc., Madison, Wisconsin, USA (2013).

[18] Bruker. *SADABS, V2012.1*, Bruker AXS Inc., Madison, Wisconsin, USA (2012).

[19] G.M. Sheldrick. *Acta Crystallogr.*, **A64**, 112 (2008).

[20] A.N. Chekhlov. *Russ. J. Inorg. Chem.*, **49**, 202 (2004).

[21] V.V. Tkachev, L.O. Atovmyan, B.V. Timikhin, O.A. Bragina, G.V. Pmtovskii, L.M. Sergienko. *J. Struct. Chem.*, **27**, 121 (1986).

[22] R.K. Harris, E.D. Becker, S.M. Cabral de Menezes, R. Goodfellow, P. Granger. *Pure Appl. Chem.*, **73**, 1795 (2001).

[23] M. Melník, M. Kabešová, M. Dunaj-Jurčo, C.E. Holloway. *J. Coord. Chem.*, **41**, 35 (1997).

[24] (a) Y. Zhang, A. Clearfield. *Inorg. Chem.*, **31**, 2821 (1992); (b) J. Le Bideau, B. Bujoli, A. Jouanneaux, C. Payen, P. Palvadeau, J. Rouxel. *Inorg. Chem.*, **32**, 4617 (1993); (c) J. Kotek, P. Lubal, P. Hermann, I. Cisarova, I. Lukes, T. Godula, I. Svobodova, P. Taborsky, J. Havel. *Chem. Eur. J.*, **9**, 233 (2003); (d) K.D. Demadis, A. Panera, Z. Anagnostou, D. Varouhas, A.M. Kirillov, I. Cisarova. *Cryst. Growth Des.*, **13**, 4480 (2013).

[25] A.N. Chekhlov. *Russ. J. Inorg. Chem.*, **49**, 243 (2004).

[26] (a) R.M.P. Colodrero, A. Cabeza, P. Olivera-Pastor, D. Choquesillo-Lazarte, A. Turner, G. Ilia, B. Maranescu, K.E. Papathanasiou, G.B. Hix, K.D. Demadis, M.G. Aranda. *Inorg. Chem.*, **50**, 11202 (2011); (b) A. Visa, B. Maranescu, A. Bucur, S. Iliescu, K.D. Demadis. *Phosphorus, Sulfur Silicon Relat. Elem.*, **189**, 630 (2014).